

Resist materials for electronic devices

Takao MIWA (三輪崇夫)

TAIYO HOLDINGS CO., LTD.

388 Ohkura, Ranzan-machi, Hiki-gun, Saitama, 355-0222, Japan

Keywords: Photolithography / Photosensitive Polyimide / Photosensitive Polybenzoxazole / DNQ / Cellulose nanofiber / TD-DFT / azo dye

1. Photosensitive polyimide (PSPI) and photosensitive polybenzoxazole (PSPBO)

PSPI^[1] and PSPBO^[2] have been used in the semiconductor industry, because of their excellent thermal stabilities, good mechanical properties, and relatively low dielectric constants. As shown in Figure 1, PSPI and PSPBO have been applied as (a) buffer coat materials, (b) interlayer insulators of re-distribution layer for wafer level packages and (c) passive components such as inductors.

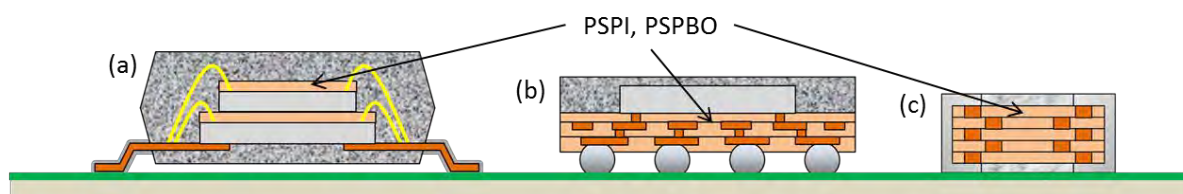


Figure 1. PSPI and PSPBO applications for electronic devices.

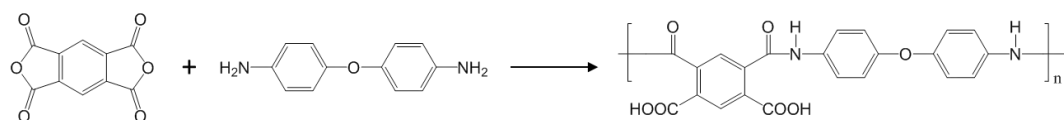
The polymer repeating unit structures of PI and PBO are shown in Figure 2.



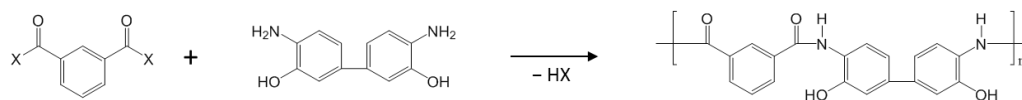
Figure 2. Chemical structures of PI and PBO.

These polymers are classified as super engineering plastics because of their excellent thermal and mechanical properties, however, show different characteristics depending on the difference in chemical structure, for example, the dielectric constant, water absorption, and cyclization temperature, which is an important selection factor in application to semiconductor devices.

In the case of using PI and PBO as the photosensitive polymer, generally, those precursors are used. The PI precursor is synthesized from a tetracarboxylic dianhydride and a diamine (scheme 1), and the PBO precursor from a dicarboxylic acid derivative and an *o*-aminophenol (scheme 2).



Scheme 1. Synthetic example of PI precursor (Polyamic acid : PAA)



Scheme 2. Synthetic example of PBO precursor (polyhydroxyamid : PHA)

Schematic representatives of photolithographic processes are shown in Figure 3.

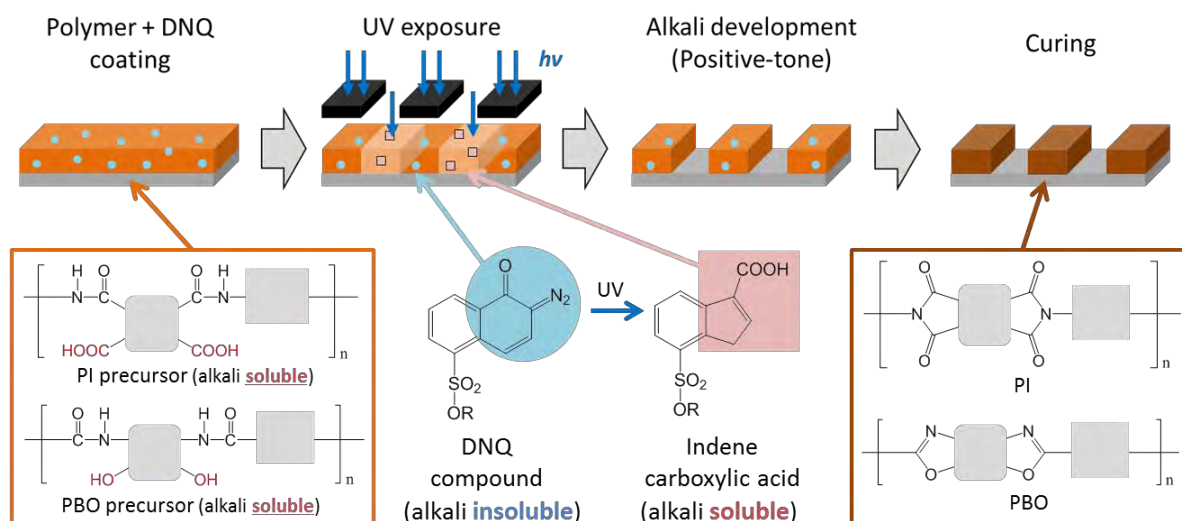


Figure 3. Photolithographic processes of positive-tone PSPI and PSPBO.

Varnish of photosensitive composition mainly containing PI or PBO precursor, DNQ (photosensitizer) and solvent is spin-coated onto a silicon wafer. After that coated film is pre-baked, exposed to a UV light through a mask so that pattern information can be transferred to the film. In the exposed area, DNQs are photo-chemically transformed to indene carboxylic acid derivatives accelerating dissolution in aqueous alkaline solutions, whereas DNQs themselves in the unexposed area are hydrophobic to inhibit solubility of matrix polymers. As a result, positive-tone pattern of PI and PBO can be obtained due to dissolution rate difference between exposed and unexposed areas in alkali developing solution and subsequent cyclization by curing.

Positive-tone PSPI and PSPBO pattern are shown in Figure 4. Good resolution and pattern shape could be seen from the SEM images.

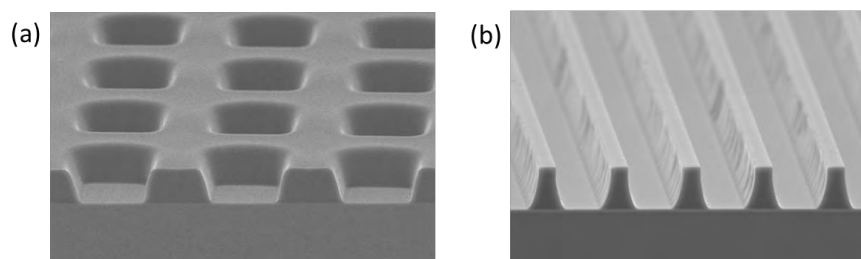


Figure 4. SEM images of positive-tone PSPI and PSPBO pattern (a) 15um hole (b) 6um line/space.

2. Cellulose nanofibers (CNFs)

CNFs have been investigated as excellent nanofiller because of their several interesting properties, for example mechanical strength, thermal stability and so on. In this study, epoxy/silica composites reinforced with CNFs were fabricated and their thermal and mechanical properties are discussed.

Epoxy/silica composites that consisted of 45 wt% silica was mixed with the CNFs solution in DMF (weight ratio of CNF was 3 wt%). The mixture solution was coat on copper foil and prebaked at 90°C for 10 min, and then backed at 180°C for 30 min. The composite materials were measured for thermal

expansion and tensile strength.

Figure 5 shows that the stress-strain curves of the epoxy/silica composites with and without CNFs. With the addition of 3 wt% CNFs, the tensile strength was improved from 91.1 MPa to 105.1 MPa, the Young's modulus was improved from 7.0 GPa to 8.0 GPa. Furthermore, it is interesting that the elongation of these composite materials at break increased in spite of the elongation of general materials with addition of CNFs is decreased.

Figure 6 shows that the relative coefficient of thermal expansion (CTE) of composite materials versus temperature. Below the glass transition temperature, CTE is decreased about 5 ppm/°C with addition of CNFs. Especially above the glass transition temperature, CTE is significantly decreased. It is indicated that CNFs suppress the Micro-Brownian motion of polymer chain.

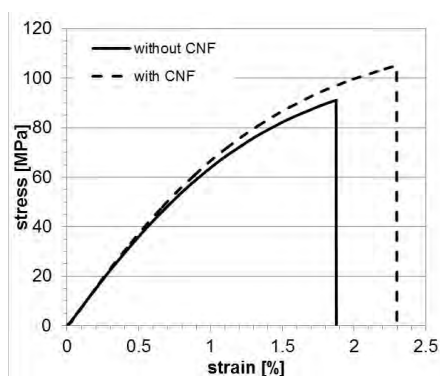


Figure. 5 Stress-strain curve of composite materials with and without CNFs.

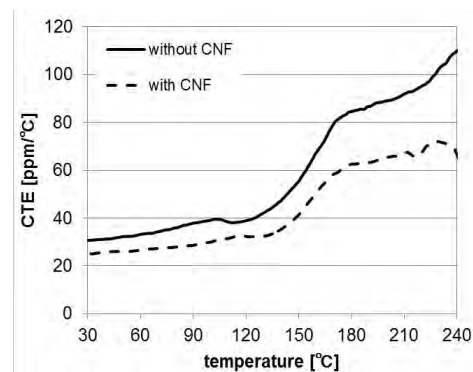


Figure. 6 Relative CTE of composite materials versus temperature.

Composite materials contained CNFs show excellent thermal and mechanical properties. The elongation at break was significantly increased and CTE was decreased. This indicated that CNFs show remarkable nanofiller effect about toughness and low CTE.

3. DFT and TD-DFT

DFT and TD-DFT calculations of azo dyes containing 2-naphthol moiety were performed. The UV-vis spectra simulation successfully reproduced the substituent effect of the azo dyes. Effect of introducing electron donating group on the HOMO and LUMO level and simulation of vibrationally-resolved electronic spectra of the dyes are discussed.

The geometry of azo dyes (Figure.7) were optimized using DFT method with B3LYP/6-311G(d,p). TD-DFT calculation for simulation of UV-vis absorption was performed to optimized structures. Vibronic structure of HOMO-LUMO transition was calculated using Franck-Condon analysis with same level as TD-DFT.

Azo dyes used in this research were shown in Figure 1. Electron donating group on their benzene ring caused red shift in UV-vis absorption. TD-DFT calculation showed same tendency and indicated the electron donating group affects mostly HOMO rather than LUMO. These dyes showed multiple peaks in solution. Franck-Condon analysis of 2-naphthol, which is partial structure of azo dyes, reproduced its shape of UV-vis spectrum. This indicates that the complex shape of absorption spectrum was due to vibronic transition. One-electron transition energies calculated from TD-DFT showed linear relationship with 0-0 transition energies obtained from peak separation(Figure.8), rather than energies at peak maxima.

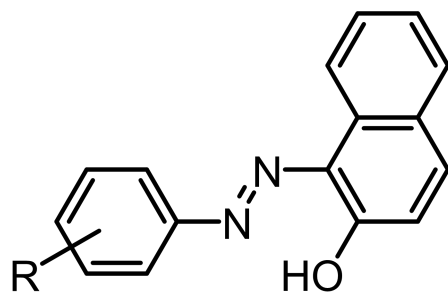
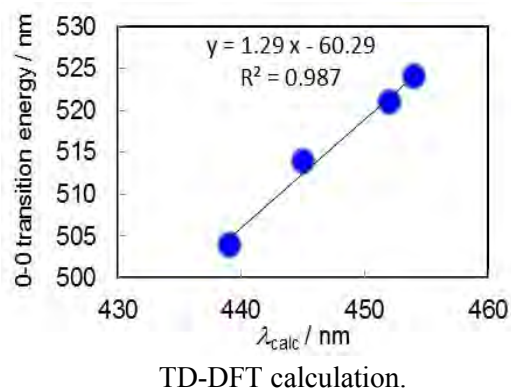


Figure.7 Azo dyes in this research

Figure.8 Relationship of 0-0 transition energy and one-electron transition energy obtained from



TD-DFT calculation.

TD-DFT calculation of azo dyes with vibronic transition was performed. Detailed investigation revealed the effect of electron donating group and linear relationship of transition energy obtained from TD-DFT and 0-0 transition energy. This indicates TD-DFT calculation can be useful for prediction of absorption edge, which is occasionally more important than absorption maximum from the view point of color.

References

- [1] K. Fukukawa, Y. Shibasaki, M. Ueda, *Polym. Adv. Technol.*, 17, 131 (2006).
 [2] T. Ogura, K. Yamaguchi, Y. Shibasaki, M. Ueda, *Polym. J.* 39, 245 (2007).

(continued from p74)

- [7] Y. W. Liu, Y. Zhang, Q. Lan, Z. X. Qin, S. W. Liu, C. Y. Zhao, Z. G. Chi, J. R. Xu, *J. Polym. Chem. Part A: Polym. Chem.*, **2013**, 51, 1302-1314.
 [8] Y. W. Liu, C. Qian, L. J. Qu, Y. N. Wu, Y. Zhang, X. H. Wu, B. Zou, W. X. Chen, Z. Q. Chen, Z. G. Chi, S. W. Liu, X. D. Chen, J. R. Xu, *Chem. Mater.*, **2015**, 27, 6547-6549.
 [9] W. X. Chen, Z. X. Zhou, T. T. Yang, R. X. Bei, Y. Zhang, S. W. Liu, Z. G. Chi, X. D. Chen, J. R. Xu, *Reactive and Functional Polymers*, **2016**, 108, 71-77.
 [10] R. X. Bei, W. X. Chen, Y. Zhang, S. W. Liu, Z. G. Chi, J. R. Xu, *Insulating Materials* (in Chinese), **2016**, 49, 1-11.R.
 [11] X. Bei, C. Qian, Y. Zhang, S. W. Liu, Z. G. Chi, X. D. Chen, J. R. Xu, M. P. Aldred, *J. Mater. Chem. C*, **2017**, 5, 12807-12815.
 [12] Y. W. Liu, Z. X. Zhou, L. J. Qu, Z. Q. Chen, Y. Zhang, S. W. Liu, Z. G. Chi, X. D. Chen, J. R. Xu, *Mater. Chem. Frontiers*, **2017**, 1, 1900-1904.